Midlatitude Sea Surface Temperature Anomalies: A Numerical Hindcast

ROBERT L. HANEY

Department of Meteorology, Naval Postgraduate School, Monterey, CA 93943

(Manuscript received 4 September 1984, in final form 19 February 1985)

ABSTRACT

A multilevel primitive equation, ocean circulation model with surface layer physics is used to study the interannual variability of sea surface temperatures (SST) in the central midlatitude North Pacific Ocean. Results from a 10-year model simulation (hindcast) driven by observed winds are analyzed and compared with observations.

The hindcast SSTs exhibit a significant amount of nonseasonal variability despite being damped toward a regular annual cycle by the thermal boundary condition at the surface. This variability is due to the horizontal and vertical redistribution of heat by currents and by parameterized turbulence processes caused by the winds. The resulting hindcast SST anomalies are correlated with observed SST anomalies at a statistically significant level over a very large part of the central midlatitude North Pacific Ocean. This suggests that wind forcing by itself, through the mechanisms noted before, makes an important contribution to the development of SST anomalies in this area. The hindcast and observed SST anomalies do not compare well in the northwest and in the southeast part of the midlatitude North Pacific, suggesting that local wind forcing by itself is relatively unimportant for SST anomaly generation in these locations.

Throughout the midlatitude North Pacific, however, the hindcast SST anomalies are only about one-third as intense as the observed anomalies. It is suggested that this discrepancy is due to the absence of forcing by anomalous surface heat fluxes in the model hindcast.

1. Introduction

In recent years, meteorologists and oceanographers have become increasingly concerned about variations in climate on monthly, seasonal, and interannual time scales. Furthermore, they have come to recognize that large-scale fluctuations in sea surface temperature (SST), i.e. SST anomalies, are an intimate part of such climate variations. As pointed out by Barnett (1981), the problem of discovering the mechanisms responsible for the creation of SST anomalies is basically a problem of attempting to close the heat budget of the upper ocean. Because of the well known difficulties associated with that problem, it is still not known for certain whether variations in net surface heat flux serve primarily to *create* SST anomalies or to *damp* them. In addition, the relative importance of winds and surface heating for the generation of SST anomalies in midlatitudes is not firmly established.

At the present time, there is some evidence to suggest that SST anomalies are generated by variations in surface heat flux on relatively short time scales, and that they are damped by heat flux variations on relatively long time scales. For example, Kraus and Morrison (1966) analyzed ocean weather ship data from the North Atlantic and North Pacific, and they found that on time scales shorter than a month, the variance of the air–sea temperature difference is primarily due to variations in the temperature of the *air,* while on time scales longer than a month, the variance is due more to variations in the temperature of the *sea.* Theoretical evidence for the earlier statement comes from a recent stochastic model study of midlatitude SST anomalies by Frankignoul and Reynolds (1983). In their model, the anomalies are generated by stochastic forcing at short time scales and they are damped by Newtonian cooling on a longer time scale. Using a nonentraining slab model of the oceanic mixed layer, Frankignoul and Reynolds were able to reproduce the frequency spectrum of observed SST anomalies over most of the midlatitude North Pacific Ocean. More importantly, the required amplitude of the stochastic forcing and the decay time of the model SST anomalies resemble observed estimates of these quantities over large parts of the North Pacific Ocean. Thus, a tentative zero-order description of SST anomalies in the frequency domain appears to be one of generation by stochastic forcing on short time scales and decay by thermal damping on longer time scales.

On the other hand, the evidence concerning the exact nature of the forcing mechanisms that are responsible for creating SST anomalies is somewhat inconclusive at the present time. This is primarily because the two major forcing fields, winds and surface heat fluxes, are highly correlated, and because present estimates of surface heat fluxes on synoptic

and monthly time scales are very uncertain (Husby, 1980; Barnett, 1981; Weare and Strub, 1981; Elsberry *et al.*, 1982; Clancy and Pollak, 1983). Thus for example, the primary lag relationship between sea level pressure (SLP) and SST anomalies found by Davis (1976, 1978) may be attributed to either anomalous Ekman advection in the ocean, or to anomalous heat fluxes at the surface. The relative importance of winds and surface heating for the generation of SST anomalies has been investigated by means of initial value experiments using numerical models (Haney *et al.*, 1978; Huang, 1979; Haney 1980). However these case studies, like earlier ones (e.g., Namias, 1972), have not demonstrated a dominant role for either of these two forcing mechanisms. More recently, Frankignoul and Reynolds (1983) used 28 years of data from the midlatitude North Pacific Ocean to compute the variance of the SST anomaly forcing due to these processes, and they found that the anomalous heat flux term was almost four times larger than the anomalous advection term. In addition to uncertainties in the estimates of surface heat flux anomalies, this result is based on the use of monthly mean winds and a very coarse grid size to compute the Ekman advection term. We therefore conclude that further studies are needed concerning the specific role of wind and surface heat fluxes in generating SST anomalies.

In the present study, the specific role of winds as a cause of SST anomalies in the central midlatitude North Pacific Ocean is investigated by means of a model hindcast. The numerical experiment is patterned after those of Busalacchi and O'Brien (1981) and Busalacchi *et al.* (1983) who used a numerical model of an idealized equatorial ocean basin to study the linear response of the equatorial Pacific Ocean to observed winds. In those studies, model pycnocline variations were compared with sea level variations observed at a number of island stations, thus providing dynamical insight into the causes of the observed sea level variability. In the present study the comparison between model and observations is focused on the SST because of its importance in air–sea interaction and climate dynamics. The ocean model and the numerical experiment are described in the next section. Results concerning the annual cycle and the anomalies are presented in the following two sections, and a summary is given at the end.

2. The model and surface forcing

The present numerical experiment makes use of the multilevel primitive equation model of Haney (1980), improved by having much greater vertical resolution and a new parameterization of surface layer physics. The horizontal grid spacing is approximately 3° longitude by 2° latitude over a closed rectangular basin extending from the equator to 65°N and from 145°E to 125°W (Fig. 1). There are 20 levels in the vertical (12 levels above 600 m) with the grid spacing increasing smoothly with depth (Fig. 2). The undisturbed depth is 4 km; the bottom is flat and the rigid-lid approximation is used. The model has nonlinear horizontal eddy viscosity and conductivity, as well as a small amount of vertical eddy viscosity (coefficient, $K_M = 5$ cm^2 s^{-1}) and conductivity (coefficient, $K_H = 0.5$ cm^2 s^{-1}) appropriate for the deep ocean. The lateral boundary conditions are those of a thermally insulated basin with zero slip everywhere except along the equatorial boundary where free slip is used.

In order to simplify the model thermodynamics, salinity has been neglected. Unfortunately, without additional model simulations, it is not possible to estimate quantitatively the effect of this simplication on the model results. In the North Pacific Ocean, salinity is certainly critical in determining the depth of the permanent pycnocline in middle and high latitudes, and fluctuations in salinity near the sea surface affect changes in the upper-ocean thermal structure (Warren, 1983). A prominent feature in previous numerical experiments (Haney, 1980) which is attributed to the neglect of salinity is an excessively deep model mixed layer during the winter season in very high latitudes. This in turn leads to an underprediction of wintertime SST variability (especially cold anomalies) in such high latitude regions. However, as argued in Sections 3 and 4, the neglect of

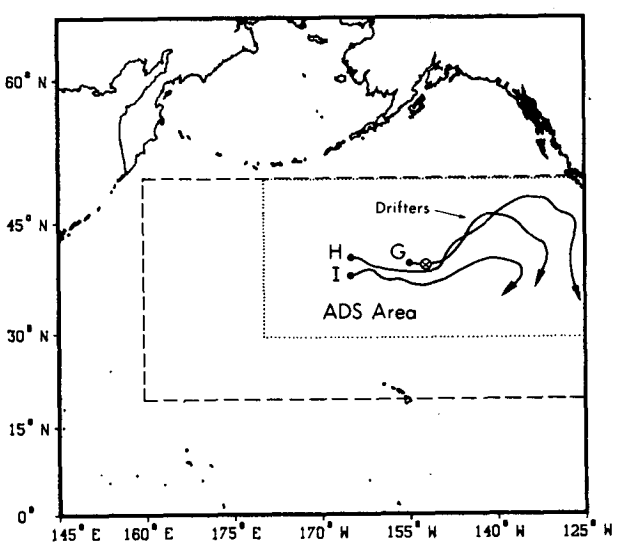

FIG. 1. The midlatitude North Pacific Ocean showing the closed rectangular domain of the model (outer boundary) and the location of the various data sets used in this study. The dashed rectangle is the region in which the model hindcast SST anomalies are compared to observed anomalies; the dotted rectangle is the Anomaly Dynamics Study (ADS) area (White and Haney, 1978); the curves labeled G, H and I are the tracks of the NORPAX drifting buoys; and the cross shows the location of the plots of the hindcast annual cycle displayed in Figs. 2–4.

salinity does not appear to have influenced the results significantly over the vast majority of the model domain south of about 45°N.

The vertical mixing of heat and momentum by surface layer processes occurs primarily as a result of a new parameterization of dynamic (shear) instability. This is done by vertically mixing both currents and temperature whenever the local gradient Richardson number (Ri) computed at the interface between model levels, falls below a critical value (presently set at 0.25). In this procedure, the temperature and velocity components at two adjacent model levels are vertically mixed in such a way that 1) heat and momentum are conserved, 2) the mixing ratios for heat and momentum are equal and 3) the value of Ri after adjustment is equal to the critical value. This procedure, hereafter referred to as dynamic adjustment (Adamec *et al.*, 1981), is quite similar to the methods of Mellor and Durbin (1975) and Pacanowski and Philander (1981) in that it produces down-gradient fluxes of heat and momentum that are very large only in regions where Ri is small. Although this parameterization is not a true embedded "mixed layer," and vertical mixing due to turbulence generated by the direct action of the wind (surface shear production) is neglected, the model results are probably not very sensitive to the particular mixed layer formulation used. As shown by Martin (1985), the most commonly used bulk and profile models of the upper ocean produce similar annual cycles of SST and mixed layer depth.

The most important model feature in the design of the numerical experiment is the method of computing the surface forcing. The surface stress and heat fluxes are computed from bulk formulae [Haney *et al.*, 1978, Eqs. (2.12)–(2.15)] using prescribed fields of atmospheric solar radiation, clouds, surface air temperature, relative humidity and winds. The surface stress is calculated using the wind-speed-dependent neutral drag coefficient [$C_D(V)$] of Large and Pond (1981), and the sensible and latent heat fluxes are calculated using exchange coefficients that are proportional to $C_D(V)$. Except for the winds, the required meteorological fields are taken from zonally averaged monthly climatologies (Haney *et al.*, 1978). The surface winds, which are used in computing the sensible and latent heat flux as well as the stress, are obtained from 6-hourly surface analyses prepared by Fleet Numerical Oceanography Center (FNOC) for the period 1969–78. See Haney *et al.* (1981) for a detailed description of the wind data, their processing and their spatial and temporal characteristics.

It is important to note that the surface heat flux computed from the above boundary condition will always be such as to couple thermally the model hindcast SST to a given (monthly climatological) apparent atmospheric equilibrium temperature (Haney, 1971). Consequently, any SST "anomaly" that might tend to develop as a result of wind forcing or other modeled dynamical processes will be thermally damped by the computed surface heat flux. The numerical experiment is therefore designed specifically to investigate nonseasonal variability which is driven by winds and damped by surface heating. The damping nature of the computed heat flux is best described using a *linearized* form of the modeled equations for the total downward surface heat flux, Q, which is

$$Q = \gamma(\mathrm{TA}^* - \mathrm{SST}). \tag{2.1}$$

Here, TA* is the apparent atmospheric equilibrium temperature, SST the model surface-layer temperature and γ a coupling coefficient which depends on a number of factors, the most important of which is the surface wind speed. With mean climatological winds $\gamma \approx 25$ W m^{-2} K^{-1} (Haney, 1971), but with the stronger synoptic winds used in the present study γ may be considerably larger, perhaps 50 W m^{-2} K^{-1}. From (2.1), the SST anomaly decay time (Frankignoul, 1979) for the present model (λ^{-1}) is given by

$$\lambda^{-1} = \rho C_p h \gamma^{-1} \tag{2.2}$$

where ρ is the density of sea water, C_p the specific heat of sea water, and h the depth of the mixed layer. With $h = 50$ m and $\gamma = 50$ W m^{-2} K^{-1}, we obtain $\lambda^{-1} = 50$ days. For shallower mixed layers and/or stronger winds, λ^{-1} will be much smaller. This value is only an approximate value however, because (2.1) is only an approximation to the surface thermal boundary condition actually used. By comparison, Frankignoul and Reynolds (1983) used $\lambda^{-1} \approx 80$ days, while Schopf (1983) used $\lambda^{-1} = 500$ days in a study of equatorial anomalies. The SST anomaly decay time is discussed further in Section 4.

The model ocean was started from a state of rest with a temperature that decreased linearly with depth. At the surface the initial temperature was equal to the annual mean value of the surface air temperature, while at the bottom it was everywhere equal to 2°C. The hindcast was started with the winds for 1 January 1974 and the integration was continued forward in time for a total of 45 years. Since only 10 years of wind data were used (1 January 1969–31 December 1978), at the end of each model decade (i.e., after 31 December 1978) the winds were reset to 1 January 1969 and the same 10 years of wind forcing were repeated. The model ocean, however, was continually advanced in time (spun-up) over the complete 45-year period of integration. This was done in order to allow sufficient time for the model upper ocean to develop its own vertical thermal structure in response to the surface heating. To reduce computer time, the first 15 years of the simulation were carried out using a grid size and time step twice as large as the one described above. The results shown below are all taken from the final decade, which is considered the true hindcast for 1969–78.

3. A typical annual cycle

In order to provide a framework for understanding and interpreting the model hindcast SST anomalies, we briefly describe a typical annual cycle in the model central midlatitude North Pacific Ocean. Any 12-month period would be sufficient for the present purpose because the year-to-year variations (anomalies) are very small compared to the annual cycle. The period from July 1976 through June 1977 is chosen for presentation because this is a time when three satellite-tracked drifting buoys were in the North Pacific Current as part of the NORPAX program (McNally *et al.*, 1983). Figures 2–4 show the time evolution of the most important variables as a function of depth at a single model grid point in midlatitude. In all the plots, significant variability on a time scale of several days to several weeks can be seen in addition to a pronounced annual cycle. This "synoptic scale" variability is the result of forcing by the observed synoptic wind field.

At 40°N, the model upper-ocean thermal structure (Fig. 2) undergoes a pronounced seasonal cycle with an annual temperature range of 9°C at the surface. The surface temperature is relatively well mixed down to a depth that varies from about 10 m in summer to more than 100 m in winter. These features compare favorably with the climatological values at this location (Robinson, 1976). At very high latitudes, because of the neglect of salinity, the model tends to predict a mixed layer depth that is considerably greater than observed. As noted above, previous numerical experiments indicate that this adverse affect of neglecting salinity is significant north of about 45°N. Since the seasonal signal in Fig. 2 compares favorably with the climatological values at this location (see also Haney *et al.*, 1978), such adverse affects do not appear to be significant in the main area of interest in middle and low latitudes.

The hindcast currents (Fig. 3) also show variability on synoptic and seasonal time scales. The strongest currents and the most pronounced variability are confined to the upper 50 m (10 m in summer). Here the current speeds vary from 10–20 cm s^{-1} in summer to 20–40 cm s^{-1} in winter. In Table 1, some of the properties of the model currents at this location are compared with those of observed currents computed from the NORPAX drifting buoys. As noted above, the time and location of the model data are specifically chosen to approximate the time and average location of the buoys (Fig. 1). The resulting comparison is quite good. Integrated over the top 23 m (AVG), the vector-averaged hindcast velocity (V) is toward the east-southeast at 10 cm s^{-1}, while the average speed (S) is 15 cm s^{-1}. Both of these values are in very good agreement with the drifter data.

However, the zonal and meridional current variances are almost twice as large in the model hindcast as in the observations. This difference exists because almost half of the variance of the near-surface currents in the model hindcast is due to inertia motion. On the other hand, inertia motion makes little or no contribution to the variance of the observed currents because the drifting buoys did not resolve such motions (McNally *et al.*, 1983). If the time series of hindcast currents are low-pass filtered to remove the inertia motion, and if the quantities in Table 1 are recomputed from the resulting low-pass filtered currents, the values of $\bar{u}$, $\bar{v}$ and V are not changed, but the average speed S, is reduced by 20 percent and the variances are reduced by 50 percent. These smaller variances, associated with motions at subinertial frequencies, compare quite favorably with the variances computed from the drifting buoys which were able

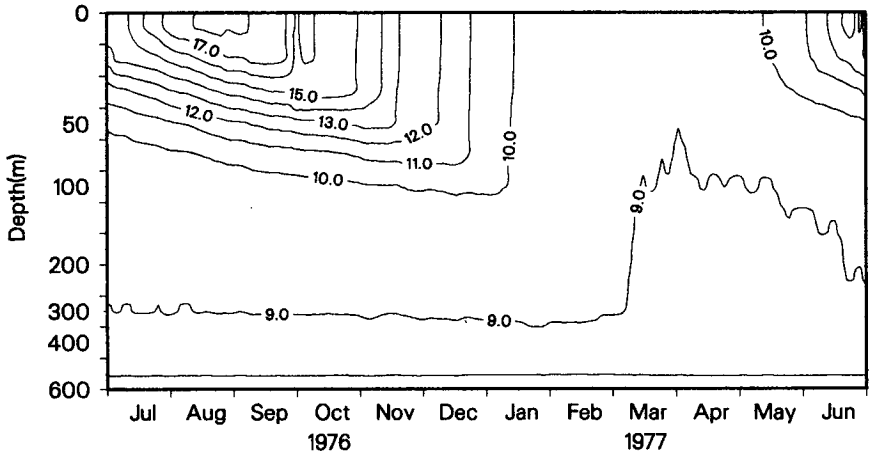

FIG. 2. Typical annual cycle of model hindcast temperatures (°C) in the central North Pacific (39°N, 152°W). Only the top 12 model levels (separated by tick marks shown on the left), extending to 600 m depth, were used to make the plot. Note the stretched vertical scale.

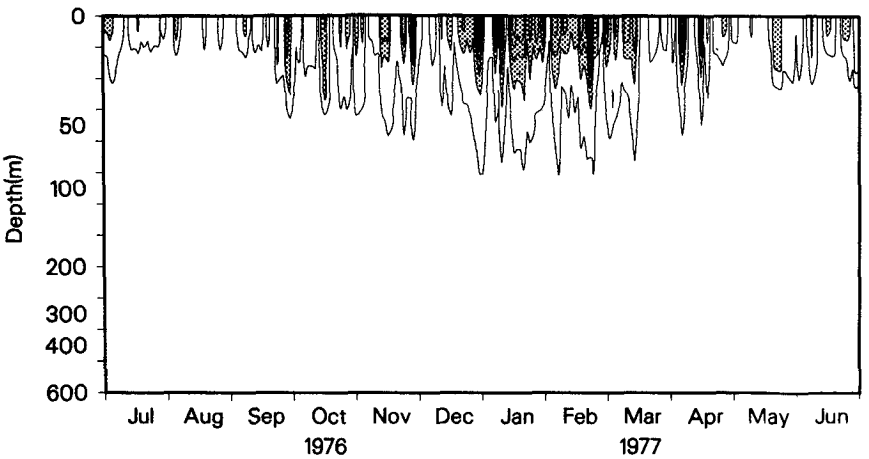

FIG. 3. As in Fig. 2 except for the current speed $[(u^2 + v^2)^{1/2}]$ in cm s^{-1} at 40°N, 152°W. The current speeds were computed from the model currents at each 3-h time step and then averaged over 36 h to produce a smoother field for plotting. Shading indicates speeds greater than 20 cm s^{-1} while the single contour is for a speed of 10 cm s^{-1}.

to detect only the larger, synoptic scales of motion. Although this comparison of currents with observations is admittedly quite limited, it suggests that the model hindcast near-surface currents are representative of the observed currents in this part of the central midlatitude North Pacific Ocean where the surface flow is primarily wind driven.

The above results can be used to make an estimate of the forcing of SST anomalies by horizontal advection of the mean temperature gradient in the model ocean. The meridional gradient of mean SST in the model ocean is a maximum in the region between 33 and 44°N where it is typically 0.01 K km^{-1}. Based on the hindcast current variances (Table 1), an appropriate value for the meridional surface current fluctuation on sub-inertial time scales is 7 cm s^{-1}. Using this value, we find

$$v' \frac{\partial}{\partial y} (\overline{SST}) \approx 7 \times 10^{-7} \text{ K s}^{-1} \qquad (3.1)$$

in the region of maximum SST gradient. This term represents the generation of SST anomalies by meridional advection of the mean SST gradient. Its variance, 5×10^{-13} K^2 s^{-2}, is considerably larger than the maximum computed by Frankignoul and Reynolds (1983) from their data.

The role of turbulent mixing in the model upper ocean can be seen from a plot (Fig. 4) of the gradient Richardson number Ri. Since the dynamic adjustment procedure was used during the integration of the model hindcast, the value of Ri in Fig. 4 cannot be subcritical. Because of the 36-hour averaging used to make the plot, values of Ri $\leq$ 1 indicate regions of enhanced vertical mixing. Sporadic mixing events of varying intensity are superposed upon a gradual deepening of the turbulent (Ri $\leq$ 1) region in fall and a more rapid shallowing of this region in spring. During this particular year, the major spring shallowing of the seasonal thermocline in the model hindcast

TABLE 1. Statistical quantities computed from the model hindcast and from drifting buoy trajectories in the North Pacific Current. The hindcast statistics are computed from the same 12-month period and model grid point shown in Fig. 3. Values are given for the top two model levels (5 m and 16 m) and for their weighted average (AVG), the latter representing the mean flow in the upper 23 m. The buoy statistics are for buoys G, H and I (McNally *et al.*, 1983; Table 2) which were drogued to 30 m in the North Pacific Ocean (Fig. 1) during approximately the same 12-month period used to compute the hindcast statistics. Shown are the mean zonal current $\bar{u}$, the mean meridional current $\bar{v}$, the magnitude of the mean current velocity $[V = (\bar{u}^2 + \bar{v}^2)^{1/2}]$, the mean speed $[S = (\overline{u^2 + v^2})^{1/2}]$, the ratio $R = V/S$, the zonal variance $(\overline{u'u'})$ and the meridional variance $(\overline{v'v'})$. Units are cm s^{-1} for velocities and cm^2 s^{-2} for variances.

Data	Depth (m)	$\bar{u}$	$\bar{v}$	V	S	R	$\overline{u'u'}$	$\overline{v'v'}$
Model hindcast	5	11.9	−4.7	12.8	19.0	0.67	309	191
(40°N, 152°W)	16	7.6	−2.5	7.9	12.0	0.66	96	74
	AVG	9.5	−3.5	10.0	15.0	0.67	189	125
Drifting buoys	G	7.4	−2.5	7.8	15.4	0.51	85	148
(35–45°N, 167–130°W)	H	9.3	−1.1	9.4	15.7	0.60	87	112
	I	9.3	−1.1	9.4	15.5	0.61	105	97

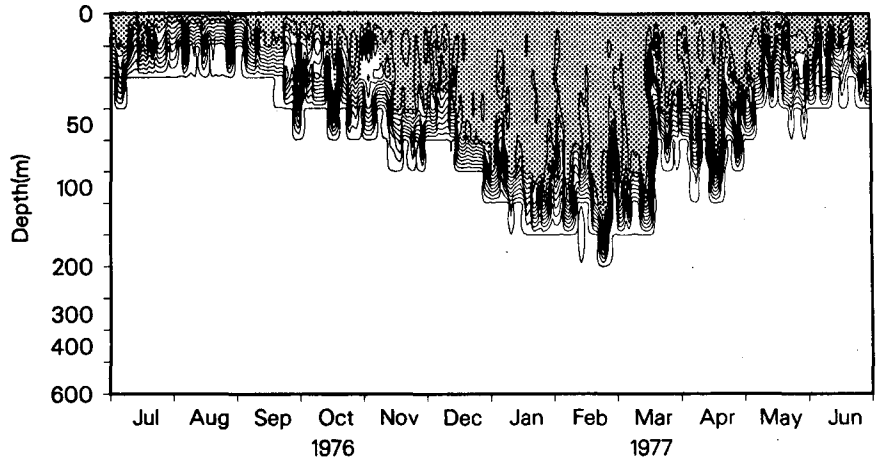

FIG. 4. As in Fig. 2 except for the gradient Richardson number (Ri) at 40°N, 152°W. Values of Ri were computed from the instantaneous model variables at each 3 h time step and then averaged over 36 h for plotting as in Fig. 3. Values less than 2.0 are shaded; values between 2.0 and 10.0 are contoured at intervals of 10.0; values greater than 10.0 (located below the "Seasonal Thermocline") are not contoured.

did not occur at this location until early May, although there was a brief, temporary shallowing in March caused by a weakening of the current shear as seen in Fig. 3.

As noted above, the use of synoptic wind forcing produces strong inertia motion in the near-surface layers of the model ocean. We have found that the vertical shear of the inertial currents makes an important contribution to the hindcast vertical turbulent mixing. This contribution can be estimated by comparing Fig. 4 with a similar plot (not shown) of Ri computed after filtering the inertia motion from the currents. Such a plot shows a somewhat smoother pattern than that in Fig. 4 and the Ri = 1 contour is about 20 m shallower during the cooling season (October–March). Thus, without the inertia motion's contribution to the vertical current shear, the depth of the quasi-isothermal layer of intense turbulent mixing in the model ocean would be considerably reduced, especially in winter.

The foregoing description is intended to document the basic state of the model ocean and to characterize its seasonal and shorter-term variability. The limited comparisons with observations suggest that the model hindcast near-surface temperature and current structure during a typical year is similar to that observed in the central midlatitude North Pacific Ocean. The focus is on the vertical and meridional thermal structure and on the near-surface current variability because these are the most important features for the development of the model hindcast SST anomalies which are analyzed in the next section. A more extensive comparison between observed and modeled climatological fields in midlatitudes using a similar model is given by Haney *et al.* (1978).

4. SST anomalies

In this section we analyze and compare the hindcast and observed SST anomalies. As described previously, such a comparison represents a model test of the importance of *wind forcing* for the development of SST anomalies in midlatitudes. All anomalies are computed from the 10 years of monthly mean data extending from January 1969 through December 1978. For both observed and hindcast data, an SST anomaly for a given month in a given year is simply the difference between the (monthly mean) SST for the given month and year, and the (monthly mean) SST for that month averaged over all 10 years. The observed SST were kindly provided by Dr. J. Namias, Scripps Institution of Oceanography, on a 5-degree latitude–longitude grid covering the North Pacific Ocean north of 20°N. The resulting anomalies were subsequently filtered by the EOF (empirical orthogonal function) method of Preisendorfer and Barnett (1977) in order to extract the large-scale geophysical signal for comparison with the hindcast anomalies. This filtering technique was previously applied to these data by Haney *et al.* (1983). The result is a "noise free" SST anomaly field which accounts for 73 percent of the variance contained in the original, unfiltered SST anomalies. Frankignoul and Reynolds (1983) also used this method to filter their SST anomaly data with very similar results. The hindcast SST anomalies were not filtered because they are considered to be "noise free" already.

As a typical example of the observed and simulated anomalies, the (seasonal) SST anomalies for the last year of the hindcast are shown in Fig. 5. During the early part of 1978 a large coherent negative anomaly

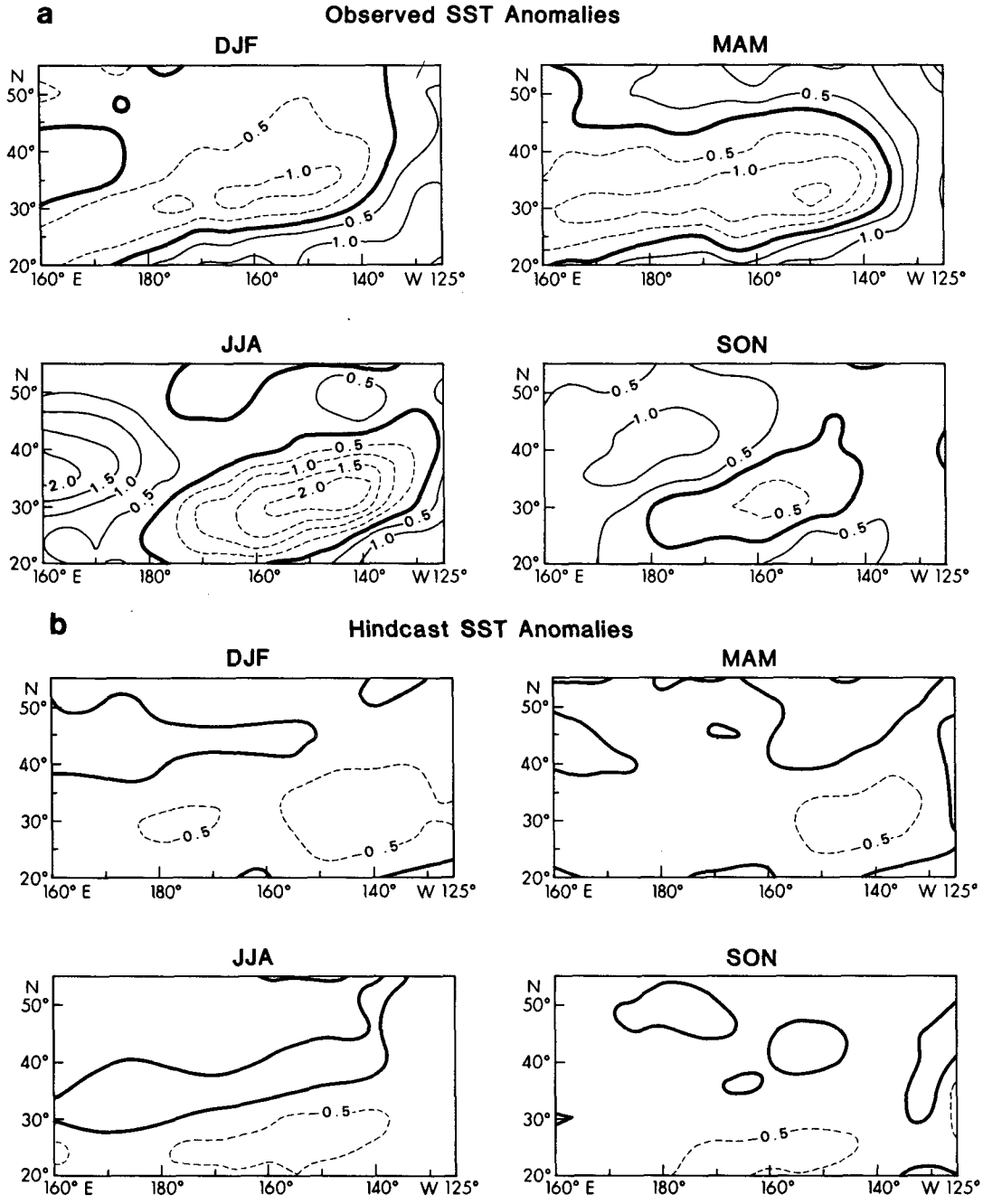

FIG. 5. (a) Observed seasonal SST anomalies for 1978, DJF is the average of December–February 1977/78; MAM is the average of March–May 1978, etc. The original data have been filtered to retain only the large-scale geophysical signal (see text). (b) As in (a) except for (unfiltered) hindcast SST anomalies.

spread slowly eastward over the central North Pacific Ocean, reaching a maximum intensity of 2°C in summer (Fig. 5a). This negative anomaly weakened rapidly in the fall, as a positive anomaly of smaller amplitude developed from the west during summer and fall. Some of these features are also seen in the hindcast SST anomalies (Fig. 5b). For example there is a negative anomaly in the central North Pacific Ocean during most of 1978, and it has a northeast–southwest orientation which is similar to that of the observed anomaly. However, the hindcast does not reproduce the warm anomaly that was observed during the latter part of 1978, and the hindcast SST anomalies are generally much weaker than the observed ones. The comparison shown in Fig. 5 is quite representative of other years as well. The patterns of

observed and hindcast SST anomalies usually show some resemblence to one another, as in Fig. 5, and the hindcast anomalies are typically much weaker than the observed ones. Even in the central midlatitude North Pacific Ocean, where wind forcing of SST anomalies is strongest, the hindcast anomalies are typically only one-third the amplitude of the observed anomalies.

Time series of hindcast and observed SST anomalies for the entire 10-year simulation at several locations in the central North Pacific are shown in Fig. 6. The top and middle graphs are from locations where the hindcast and observed SST anomalies are correlated the best (Fig. 7). Variability on a range of time scales is evident in both the observed and hindcast time series. While the *amplitude* of the hindcast anomalies

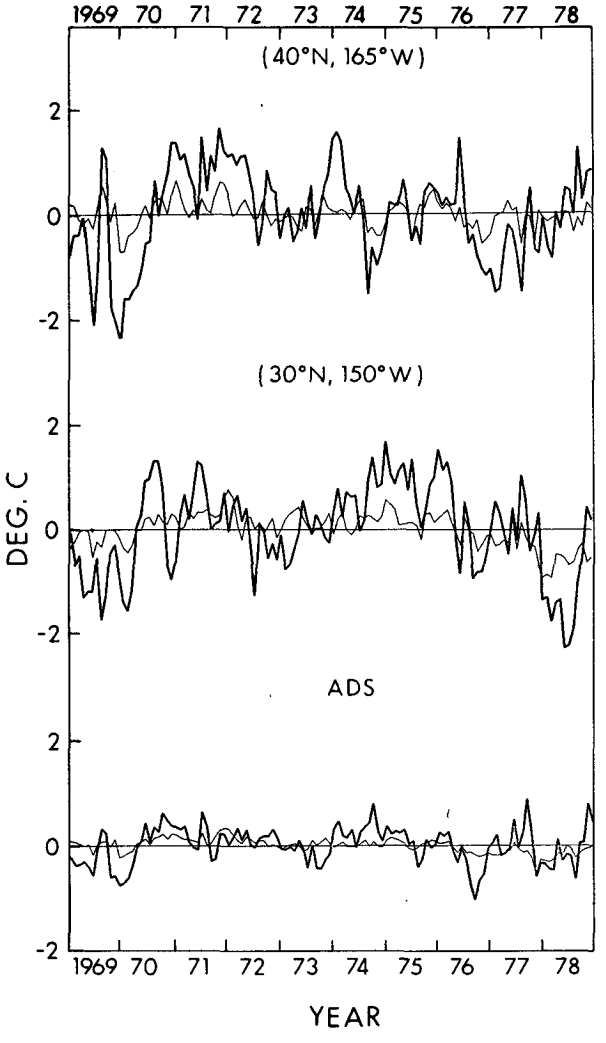

FIG. 6. Time series of observed (thick lines) and hindcast (thin lines) SST anomalies. The top and middle graphs are SST anomalies at the latitude and longitude shown, while the bottom graph is the SST anomalies averaged over the ADS area (Fig. 1).

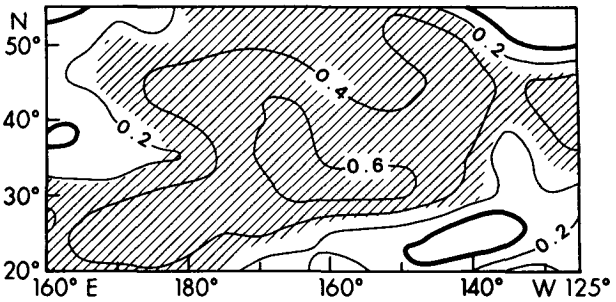

FIG. 7. Correlation coefficient computed from the 10-year time series of observed and hindcast SST anomalies at each grid point. The region where the correlation coefficient is positive at the 95 percent significance level is shaded.

is clearly much smaller than that of the observed anomalies, the *timing* and *relative* amplitude of the observed and hindcast anomalies are quite similar. Thus for example, at 40°N, 165°W the model hindcast produced major negative anomalies in 1970, 1974–75, and 1976–77, and major positive anomalies in 1971–72, 1974, and 1976. These features, as well as similar ones in the time series at 30°N, 150°W and in the ADS area (White and Haney, 1978) coincide quite closely with features in the corresponding observed time series. This general agreement between the hindcast and observed SST anomaly time series suggests that most of the major SST anomalies at these locations during 1969–78 can be explained, in part, by local wind forcing only. The discrepancy between the *amplitude* of the hindcast and observed anomalies is examined below. It is worth noting that all the time series in Fig. 6 are from regions of the North Pacific Ocean where the mean winds are strong and wind variability is large (Haney *et al.*, 1981; Haney *et al.*, 1983). This is where wind forcing clearly has the greatest *potential* for contributing to SST anomaly development.

The comparison between hindcast and observed SST anomalies over the entire North Pacific is revealed by the correlation coefficients and their significance levels shown in Fig. 7. As can be seen, the two fields are positively correlated at a statistically significant level over a large part of the central midlatitude North Pacific Ocean. The correlations are insignificant in the northwest and southeast parts of the North Pacific. The statistical significance of the correlation coefficients shown in Fig. 7 can be estimated by normalizing the raw values by the large lag standard error (σ) computed from the two data sets being correlated (Sciremammano, 1979). The values of σ computed from the observed and hindcast SST anomalies (not shown) are fairly uniform over the midlatitude North Pacific with an average value of 0.12. Correlation coefficients greater than 4σ cover a sizeable area in Fig. 7. Values greater than $2\sigma \approx 0.24$ cover much of the central North Pacific, and these

are positive at the 95 percent confidence level. As seen in Fig. 6 however, even in these regions where the correlations are highest, the hindcast SST anomalies are much weaker than the observed anomalies.

The correlations in Fig. 7 are interpreted as follows. In the model hindcast, SST anomalies are generated only when fluctuations in the winds produce anomalous currents or turbulent vertical mixing which then redistributes the existing (horizontal and vertical) temperature structure. This must be true in the model because, as described in Section 2, the heat flux at the sea surface always acts to *damp* any SST anomaly that forms. This mechanism is expected to be important in the real ocean also, but only in those regions where large variations in wind, and large gradients in temperature exist simultaneously. These are the regions where the hindcast SST anomalies and the observed SST anomalies are best correlated. The largest and most significant correlations occur in the central North Pacific Ocean along and to the southeast of the major midlatitude storm tracks. This is also where Haney *et al.* (1983) found a statistically significant relationship between monthly anomalies of U_*^3 (surface friction velocity cubed), computed from 6-hourly synoptic wind fields, and monthly anomalies of SST. The pattern of large correlations in Fig. 7 is therefore physically realistic as well as statistically significant. The low correlations in the northwest part of the North Pacific may be due in part to the effects on SST anomalies of eddies and meanders associated with the Kuroshio Extension. Such eddy motions are not resolved in the present hindcast because of the coarse grid size used. The low correlations in the southeast part of the North Pacific are attributed to the fact that this is a region of relatively light winds year-round. Wind forcing cannot be an important factor in regions where the winds themselves are weak. Excluding these two relatively small regions of low correlations, the results shown here provide clear modeling evidence that wind forcing by itself plays a significant role in the development of large-scale SST anomalies in a large part of the central midlatitude North Pacific Ocean.

Although a general analysis of subsurface anomalies is beyond the scope of the present study, the vertical structure of the hindcast temperature anomalies at a single grid-point in the model North Pacific is shown in Fig. 8. The grid point is located in the region where the hindcast and observed SST anomalies are highly correlated. It can be seen that the most significant temperature anomalies are confined to the upper 50–100 m which is also where the largest hindcast temperature gradients and current variabilities are located (Figs. 2 and 3). Some of the anomaly structures are characteristic of vertical mixing "events," e.g., a weak negative anomaly at the surface with a stronger positive anomaly immediately below it, as in 1976 and 1978. Others are more coherent from the surface to 100 m. In either case however, in the midlatitude region where the observed and hindcast SST anomalies are well correlated, the hindcast anomalies are clearly associated with thermal structures that are largely confined to the surface layer. This result is consistent with the findings of Barnett (1981) who analyzed 45 monthly AXBT sections taken in the central North Pacific (along 158 and 170°W between 30 and 50°N) during a 4-year period (1974–77) included within the present 10-year hindcast period. We therefore see that in the central North Pacific Ocean, the hindcast temperature anomalies not only correlate well with observations at the surface, but they also have a vertical scale that is similar to that which is observed.

Even in the central North Pacific Ocean, where the hindcast and observed SST anomalies are well correlated and their subsurface expressions have similar vertical scales, the hindcast anomalies are much weaker than the observed anomalies (Fig. 6). This discrepancy can also be seen in the power spectra of these time series which are shown in Fig. 9. Over the

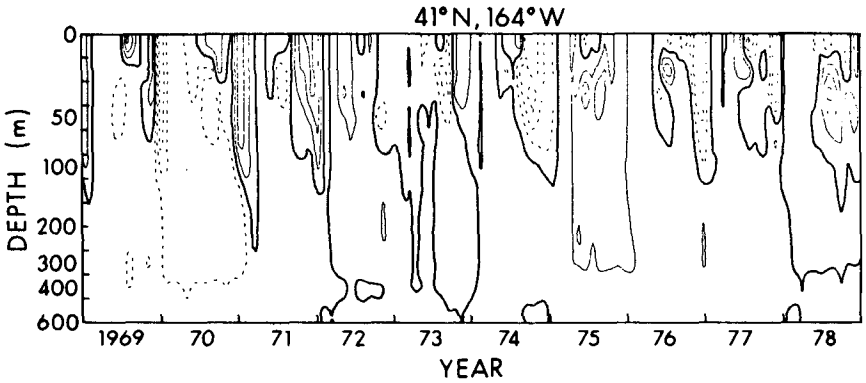

FIG. 8. Model hindcast temperature anomalies from the central North Pacific Ocean as a function of depth and time. The contour interval is 0.2°C, with the zero contour heavy, positive contours solid and negative contours dashed.

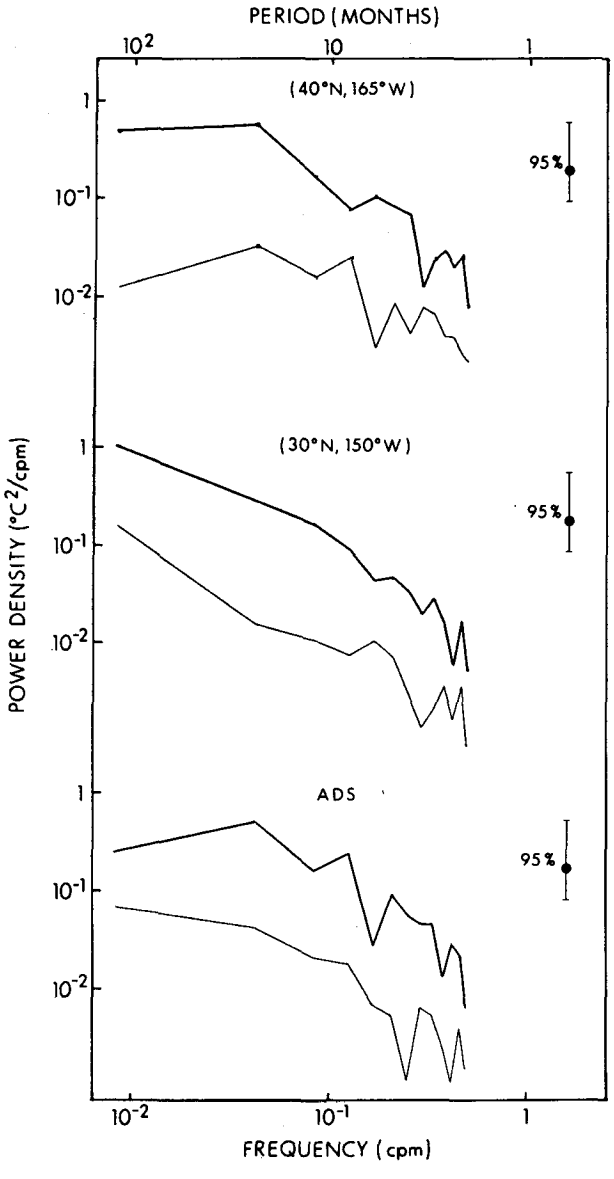

FIG. 9. Power spectrum of observed (thick lines) and hindcast (thin lines) SST anomalies at the same locations as the time series in Fig. 6.

range of periods from two months to 120 months, the model hindcast consistently underpredicts the power density of the observed SST anomalies. The discrepancy is approximately an order of magnitude at all frequencies except for the very lowest frequencies where it is even greater. It follows that the total *variances* of the two fields differ by approximately an order of magnitude, and that the *standard deviation* of the hindcast SST anomalies is only about *one-third* the standard deviation of the observed anomalies. It is important to note however that the spectrum of the observed and hindcast SST anomalies in Fig. 9 have essentially the same *shape*.

5. Discussion

We now attempt to answer the basic question addressed by this study. The question is whether or not wind forcing by itself is the cause of SST anomalies in midlatitudes. For the sake of the argument, suppose that the observed SST anomalies are in fact due only to the redistribution of heat in the upper ocean caused exclusively by wind forcing. Since the wind driven hindcast model underpredicts the observed SST anomaly amplitude by approximately a factor of 3, this discrepancy between the observed and hindcast SST anomaly amplitudes would have to be due to some kind of major deficiency in the hindcast model itself. We now examine a number of potential model deficiencies to see if they can account for such a discrepancy.

Consider first the possibility that the magnitude of the wind stress forcing is too weak. In the model hindcast the surface stress is computed from 6-hourly synoptic wind fields using a wind speed-dependent drag coefficient. Furthermore, the hindcast variables most directly related to the surface stress, the mean and fluctuating surface currents, compare favorably with observations (Table 1). In addition, the mean horizontal and vertical temperature gradients in the model hindcast also compare favorably with observations (Section 3). An exception occurs at high latitudes in winter where the model vertical stratification is too weak owing to the neglect of salinity. However, since the SST anomalies are underpredicted as much at 20°N (where salinity is not a critical factor) as at 40°N (Fig. 9), this discrepancy does not seem to be attributable to the neglect of salinity in the model. From these considerations we conclude that the large discrepancy between the hindcast and observed SST anomaly amplitudes is not likely to be due to unrealistically weak wind stress forcing or weak internal temperature gradients in the hindcast model.

Another potential explanation for the discrepancy between the magnitude of the hindcast and observed SST anomalies is the fact that vertical mixing due to turbulence generated by surface shear production is neglected in the model. The effect of such turbulent vertical mixing can be parameterized by an entrainment term proportional to U_*^3/h^2 in the equation for mixed layer temperature (Kraus and Turner, 1967). An entrainment term of this type is strongly dependent on the magnitude of the wind stress, and therefore it can produce a sizeable SST response to wind forcing. While a complete analysis of the effect that such an additional term would have on the present hindcast results is beyond the scope of this study, it is certainly not obvious that the effect would be a significant increase in the hindcast SST anomaly amplitude. In fact, it is very likely that a large part of the "new" vertical mixing which would occur as a result of

adding such a term to the hindcast model would simply end up *replacing*, rather than adding to, the wind generated vertical mixing which presently occurs through the dynamic adjustment mechanism. This is suggested by the fact that different upper-ocean mixed layer models give relatively similar results even though they are based on rather different principles (Martin, 1985). If that were to happen, the intensity of the hindcast SST anomalies would not be increased at all by the addition of the new term. As a result, it does not seem that this potential explanation can actually account for the factor-of-3 discrepancy between the observed and hindcast SST amplitudes. From the foregoing considerations, we conclude that the discrepancy is not likely to be due to processes by which the hindcast SST anomalies are *generated* by the wind stress forcing.

Consider now the processes by which the SST anomalies are *damped* in the model hindcast. A simple estimate of the time scales associated with the horizontal and vertical eddy diffusion of heat shows that these processes are entirely negligible compared to the damping by the surface thermal boundary condition. A careful analysis, however, shows that damping by the surface thermal boundary condition is not likely to be the cause of the discrepancy between hindcast and observed SST anomaly amplitudes. This is because the anomaly decay time (λ^{-1}) has a relatively small effect on the amplitude of the anomalies, but it has a relatively large effect on their phase. A change in λ^{-1} that would increase the amplitude of the SST anomalies by a factor of 3 would completely destroy the relatively good phase relationship (correlations) that exists in the present hindcast results. This can be shown quite easily using theory from the stochastic forcing model (which is considered to be a zero-order approximation to the present hindcast model). Here one finds that

$$\int F_T(\omega)d\omega = F_v(0)\int (\omega^2 + \lambda^2)^{-1}d\omega = \frac{\pi}{2}F_v(0)\lambda^{-1}, \quad (5.1)$$

where ω is the frequency, $F_T(\omega)$ is the SST anomaly spectrum, and $F_v(0)$ is the level of the atmospheric forcing spectrum in a suitable frequency range (Frankignoul, 1979). The left side of (5.1) is the SST anomaly variance, and the equation shows that λ^{-1} would have to be increased by a factor of 10 in order for it to increase the hindcast SST anomaly variance by the order of magnitude that is needed to account for the present discrepancy. At the same time, the phase (ϕ) between the SST anomalies and the forcing is given by

$$\phi = -\arctan(\omega\lambda^{-1}). \quad (5.2)$$

From (5.2) we find that if λ^{-1} were increased by a factor of 10, the phase of the hindcast SST anomalies that have periods of the order of several months (the present value of λ^{-1}, say) would be changed significantly. This would clearly alter the good phase agreement, i.e., correlation, that presently exists between the hindcast and observed SST anomalies (Figs. 6 and 7). Furthermore, the present estimate of $\lambda^{-1} \approx 50$ days is in good agreement with the value needed in order for the stochastic forcing model to fit the SST anomaly spectrum at various weather stations (Frankignoul, 1979) and over the central North Pacific Ocean (Frankignoul and Reynolds, 1983). This consistency between the two estimates of λ^{-1}, one essentially from observations (Haney, 1971) and the other from the stochastic forcing models, was pointed out earlier by Gill (1979). From the above considerations, we conclude that the discrepancy between the amplitude of the hindcast and observed SST anomalies is not likely to be due to unrealistically strong damping by the surface thermal boundary condition used in the hindcast model.

In the previous paragraphs, we have supposed that observed SST anomalies in midlatitudes are in fact produced only by wind forcing, and we have searched for a deficiency in the model hindcast that could account for the wind driven model's failure to reproduce the observed SST anomaly variance. We have essentially ruled out the potential deficiencies of weak wind forcing, weak internal temperature gradients, and excessive thermal damping at the surface. Our analysis and model results therefore lead us to conclude that observed SST anomalies in the central North Pacific are not caused by wind forcing alone. That is, we conclude that the hindcast model is reproducing the actual ocean's response to wind forcing (to at least a factor-of-3 accuracy), and that this response fails to account for the observed SST anomaly amplitude.

The above model results strongly suggest that anomalous surface heat fluxes are essential for the generation and maintenance of large-scale SST anomalies in midlatitudes. Winds alone simply can not do it. Yet, as is apparent from (5.1), an additional forcing term of sufficient magnitude, such as anomalous surface heat fluxes, is quite capable of increasing the SST anomaly variance. This result is consistent with that of Frankignoul and Reynolds (1983) who came to essentially the same conclusion about the dominance of anomalous heat flux forcing of SST anomalies in midlatitudes by an entirely different method. As described previously, their result is based on comparing the variance of observed estimates of anomalous surface heat fluxes with the variance of observed estimates of Ekman advection computed from monthly mean wind fields and observed temperature gradients.

Since the observed and modeled SST anomalies are generally in phase (Fig. 6) and thus positively correlated (Fig. 7), the anomalous heat fluxes that are

required to account for the observed SST anomaly amplitude would have to be in phase in time and space with the wind induced effects. Typical meteorological situations in which this is thought to occur include those of weak wind mixing, reduced sensible and latent heat losses and increased solar heating in calm, cloud-free areas of high atmospheric pressure, and the opposite in regions of storms and low pressure. Wind-induced advective effects in the upper ocean are also correlated with heat flux anomalies. For example, northwest winds at the surface, which tend to reduce the SST in midlatitudes through horizontal Ekman advection in the ocean, are usually advecting colder and drier air, resulting in a greater heat loss from the sea surface. It is precisely this correlation between wind effects and surface heat flux effects, and the resulting difficulty in separating the two through observations, that provided the major motivation for this study.

6. Summary and conclusions

The large-scale thermal response of the midlatitude North Pacific Ocean to a long history of observed winds was modeled and compared with observations. The thermal forcing at the surface was such as to damp the model SST toward a regular annual cycle. The numerical experiment was thus a model investigation of the role of wind forcing for the generation of SST anomalies in midlatitudes. The separate role of wind forcing is not easily determined from observations alone because surface winds and surface heat fluxes are correlated, and present estimates of surface heat fluxes are highly unreliable.

The model hindcast reproduces the major observed features of the upper-ocean thermal structure and current variabilities. In addition to simulating a realistic north–south SST gradient, a direct result of the thermal forcing at the surface, the hindcast also reproduced the typical seasonal cycle of mixed layer depth and vertical temperature gradient in the upper ocean. Near-surface currents in the model central North Pacific Ocean compare well with estimates of the observed currents obtained from the NORPAX drifting buoys.

The model hindcast SST anomalies are positively correlated with observations at a statistically significant level over most of the central midlatitude North Pacific Ocean. Regions where the correlations are not significant are in the Northwest Pacific, perhaps owing to the effect on SST anomalies of the near-surface eddy field associated with the Kuroshio Extension, and in the southeast part of the North Pacific, where wind forcing is generally light all year. In the central North Pacific, the hindcast temperature anomalies are largely confined to the mixed layer, in agreement with Barnett's (1981) analysis of four years of AXBT data from the same area.

Although the hindcast and observed SST anomalies are highly correlated, the hindcast anomalies are much weaker than the observed ones. The power spectrum of hindcast and observed SST anomalies shows that the model reproduces the *shape* but not the *amplitude* of the observed spectrum. From theoretical considerations derived from the stochastic-forcing model of climate variability, it is suggested that the most likely cause of the discrepancy between the hindcast and observed SST anomaly amplitude is the absence of forcing by anomalous surface heat fluxes in the hindcast experiment. This result is consistent with that of Frankignoul and Reynolds (1983) who computed the variance of SST anomaly forcing due to anomalous surface heat fluxes and found it to be several times larger than that due to horizontal advection by wind driven Ekman transport. This means that if we are to improve our understanding of interannual variability of SST in midlatitudes, reliable estimates of the anomalous surface heat fluxes are required. Fortunately for this problem, there has been some recent progress which indicates that improved estimates of some of the heat flux components may in fact be achievable by remote-sensing techniques in the not too distant future (Gautier, 1981; Liu and Niiler, 1984).

Acknowledgments. I am especially grateful to FNOC for providing the surface wind data and to Jerome Namias for providing the SST data used in the present study. I would also like to thank R. Elsberry, R. Garwood, L. Magaard, P. Muller and K. Wyrtki for valuable discussions during the course of this study. This work was completed during a one-year sabbatical at the University of Hawaii, and I would like to thank my host, Lorenz Magaard, for helping to make my sabbatical such a rewarding experience.

Computer time was provided by the W. R. Church Computer Center at the Naval Postgraduate School. This research was supported by the Office of Naval Research (Contract N0001484AF00001) as part of the NORPAX program. This support is gratefully acknowledged.

REFERENCES

Adamec, D., R. L. Elsberry, R. W. Garwood, Jr. and R. L. Haney, 1981: An embedded mixed layer-ocean circulation model. *Dyn. Atmos. Oceans,* **5,** 69–96.

Barnett, T. P., 1981: On the nature and causes of large-scale thermal variability in the central North Pacific Ocean. *J. Phys. Oceanogr.,* **11,** 887–904.

Busalacchi, A. J., and J. J. O'Brien, 1981: Interannual variability of the equatorial Pacific in the 1960's. *J. Geophys. Res.,* **86,** 10 901–10 907.

——, K. Takeuchi and J. J. O'Brien, 1983: Interannual variability of the equatorial Pacific—revisited. *J. Geophys. Res.,* **88,** 7551–7562.

Clancy, R. M., and K. D. Pollak, 1983: A real-time synoptic ocean thermal analysis/forecast system. *Progress in Oceanography,* Vol. 12, Pergamon, 383–424.

Davis, R. E., 1976: Predictability of sea surface temperature and sea level pressure anomalies over the North Pacific Ocean. *J. Phys. Oceanogr.*, **6**, 249–266.

——, 1978: Predictability of sea level pressure anomalies over the North Pacific Ocean. *J. Phys. Oceanogr.*, **8**, 233–246.

Elsberry, R. L., P. C. Gallacher, A. A. Bird and R. W. Garwood, Jr., 1982: Deriving corrections to FNOC surface heat flux estimates for use in North Pacific Ocean prediction. Naval Postgraduate School Tech. Rep. NPS 63-82-005, 68 pp.

Frankignoul, C., 1979: Stochastic forcing models of climate variability. *Dyn. Atmos. Oceans*, **3**, 465–479.

——, and R. W. Reynolds, 1983: Testing a dynamical model for midlatitude sea surface temperature anomalies. *J. Phys. Oceanogr.*, **13**, 1131–1145.

Gautier, C., 1981: Daily short wave energy budget over the ocean from geostationary satellite measurements. *Oceanography from Space*, J. F. R. Gower, Ed., Plenum, 201–206.

Gill, A. E., 1979: Comments on stochastic models of climate variability. *Dyn. Atmos. Oceans*, **3**, 481–483.

Haney, R. L., 1971: Surface thermal boundary condition for ocean circulation models. *J. Phys. Oceanogr.*, **1**, 241–248.

——, 1980: A numerical case study of the development of large-scale thermal anomalies in the central North Pacific Ocean. *J. Phys. Oceanogr.*, **4**, 541–556.

——, W. S. Shiver and K. H. Hunt, 1978: A dynamical-numerical study of the formation and evolution of large-scale ocean anomalies. *J. Phys. Oceanogr.*, **8**, 952–969.

——, M. S. Risch and G. C. Heise, 1981: Wind forcing due to synoptic storm activity over the North Pacific Ocean. *Atmos. Ocean*, **19**, 128–147.

——, B. H. Hautman and W. H. Little, 1983: The relationship between wind and sea surface temperature anomalies in the midlatitude North Pacific Ocean. *Atmos. Ocean*, **21**, 168–186.

Huang, J. C. K., 1979: Numerical case studies for oceanic thermal anomalies with a dynamical model. *J. Geophys. Res.*, **84**, 5717–5726.

Husby, D. M., 1980: A comparison of surface heat flux estimates from ocean weather station V and merchant vessels in its vicinity in the western North Pacific region, 1956–1970. *J. Phys. Oceanogr.*, **10**, 971–975.

Kraus, E. B., and R. E. Morrison, 1966: Local interactions between the sea and the air at monthly and annual time scales. *Quart. J. Roy. Meteor. Soc.*, **92**, 114–127.

——, and J. S. Turner, 1967: A one-dimensional model of the seasonal thermocline. II: The general theory and its consequences. *Tellus*, **19**, 98–106.

Large, W. G., and S. Pond, 1981: Open ocean momentum flux measurements in moderate to strong winds. *J. Phys. Oceanogr.*, **11**, 324–336.

Liu, W. T., and P. P. Niiler, 1984: Determination of monthly mean humidity in the atmospheric surface layer over the oceans from satellite data. *J. Phys. Oceanogr.*, **14**, 1451–1457.

Martin, P. J., 1985: Simulation of the mixed layer at OWS November and Papa with several models. *J. Geophys. Res.*, **90**, 903–916.

McNally, G. J., W. C. Patzert, A. D. Kirwan, Jr. and A. C. Vastano, 1983: The near-surface circulation of the North Pacific using satellite tracked drifting buoys. *J. Geophys. Res.*, **88**, 7507–7518.

Mellor, G. L., and P. A. Durbin, 1975: The structure and dynamics of the ocean surface mixed layer. *J. Phys. Oceanogr.*, **5**, 718–728.

Namias, J., 1972: Experiments in objectively predicting some atmospheric and oceanic variables for the winter of 1971–72. *J. Appl. Meteor.*, **11**, 1164–1174.

Pacanowski, R. C., and S. G. H. Philander, 1981: Parameterization of vertical mixing in numerical models of tropical oceans. *J. Phys. Oceanogr.*, **11**, 1443–1451.

Preisendorfer, R. W., and T. P. Barnett, 1977: Significance tests for empirical orthogonal functions. *Preprints Fifth Conf. on Probability and Statistics in Atmospheric Sciences*, Las Vegas, Amer. Meteor. Soc., 169–172.

Robinson, M. K., 1976: *Atlas of North Pacific Ocean Monthly Mean Temperatures and Mean Salinities of the Surface Layer.* NOORP-2, Naval Oceanographic Office, Washington, DC, 194 pp.

Schopf, P. S., 1983: On equatorial waves and El Nino. Part II: Effects of air–sea thermal coupling. *J. Phys. Oceanogr.*, **13**, 1878–1893.

Sciremammano, F., Jr., 1979: A suggestion for the presentation of correlations and their significance levels. *J. Phys. Oceanogr.*, **9**, 1273–1276.

Warren, B. A., 1983: Why is no deep water formed in the North Pacific? *J. Mar. Res.*, **41**, 327–347.

Weare, B. C., and P. T. Strub, 1981: The significance of sampling biases on calculated monthly mean oceanic surface heat fluxes. *Tellus*, **33**, 211–224.

White, W. B., and R. L. Haney, 1978: The dynamics of ocean climate variability. *Oceanus*, **21**, 33–39.